Proc. 13th International Beam Instrumentation Conference,Beijing JACoW Publishing
ISBN: 978-3-95450-249-3 ISSN: 2673-5350 doi: 10.18429/JACoW-IBIC2024-THP60

MACHINE LEARNING USED IN BPM DISPLACEMENT PREDICTION AT HLS II*

C. H. Wang, D. Y. Wang, J. K. Lan, M. D. Ma, T. Y. Zhou†, B. G. Sun
NSRL, University of Science and Technology of China, Hefei, Anhui 230029, China

Abstract

Beam orbit stability is a crucial indicator that can be used to evaluate the performance of a synchrotron radiation source. It can be improved through precise orbit measurement with beam position monitors (BPMs) and appropriate orbit feedback. The movement of BPMs directly affects the measurement of the beam orbit and indirectly affects the beam orbit through orbit feedback (OFB) system. Two sets of BPM displacement measurement system were established at Hefei Light Source II (HLS II) storage ring and some machine learning work was carried out on the system.

INTRODUCTION

Hefei Advanced Light Source (HALF), under construction by National Synchrotron Radiation Laboratory, is a fourth-generation storage ring. In order to realize the beam orbit stability of HALF, relevant studies have been performed on HLS II. In general, the beam orbit stability is required to be less than 10% of the beam size [1, 2].

The mechanical stability of BPM can be affected by both ambient environment sources and machine-inherent source [3]. The influence of BPM mechanical stability on beam position measurement is shown in Fig. 1. The BPM displacement x_d is numerically equal to the difference between the actual BPM reading x_{BPM} and real beam position x_{beam}, as shown in Eq. (1).

$$x_{beam} = x_{BPM} - x_d. \quad (1)$$

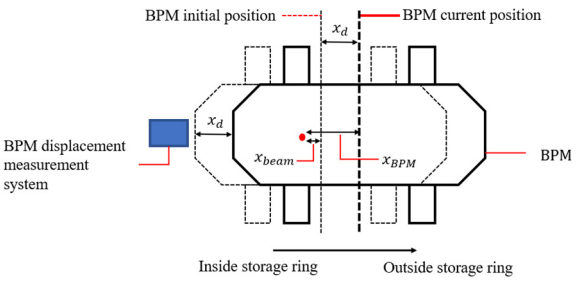

Figure 1: Model of BPM movement.

The influence of BPM displacement x_d on beam orbit can be calculated by Accelerator Toolbox (AT) in MATLAB with the linear lattice of HLS II as shown in Fig. 2. The related parameters of the HLS II storage ring are shown in Table 1. Random displacement of normal distribution $N(\mu = 0, \sigma^2 = \Delta x^2 \text{ or } \Delta y^2)$ with different Δx and Δy is added to the 32 BPMs in HLS II lattice AT file and the closed orbit distortion (COD) with orbit feedback being activate is calculated. The calculation result is shown in Fig. 3(a) and (b). After linear fitting, we have $\frac{d\ rms\ COD_x}{d\ rms\ \Delta x} = 0.907$, $\frac{d\ rms\ COD_y}{d\ rms\ \Delta y} = 0.940$, $\frac{d\ rms\ COD_x}{d\ rms\ \Delta y} = 0$, $\frac{d\ rms\ COD_y}{d\ rms\ \Delta x} = 0$.

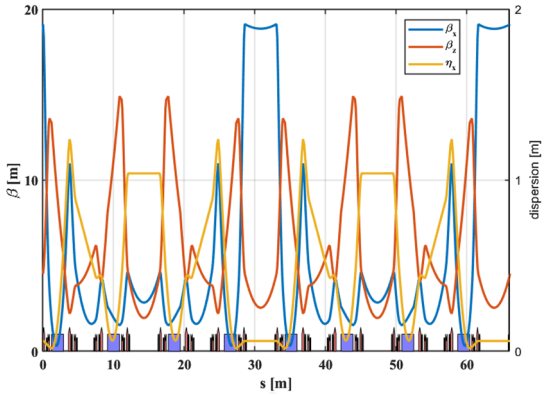

Figure 2: Schematic of the HLS II linear lattice.

Table 1: Parameters for the HLS II Storage Ring

Parameter	unit	HLS II
Circumference	m	66.131
Energy	GeV	0.8
RF frequency	MHz	204
Harmonic number	/	45
Horizontal beam size	μm	≥400
Vertical beam size	μm	≥83
Horizontal tune	/	4.445
Vertical tune	/	2.360
Lattice number	N	2

In general, the beam orbit stability is required to be less than 10% of the beam size [1, 2]. Based on the premise of considering only the influence of the BPM movement, to achieve beam orbit stability (10% beam size) for HLS II, the rms BPM displacement should be less than 44.101 μm in the horizontal plane and 8.830 μm in the vertical plane.

SYSTEM INSTALLATION

Two sets of capacitive displacement measurement systems from Micro-Epsilon [4] were installed at P1 and P2 in HLS II storage ring as shown in Fig. 4. The measurement result is shown in Fig. 5.

* Work supported by the National Natural Science Foundation of China under Grant No.12005223, 12075236 and the Hefei Advanced Light Facility Pre-research Project, and the Hefei Advanced Light Facility Project.
† tianyuzhou@ustc.edu.cn

ISBN: 978-3-95450-249-3 ISSN: 2673-5350 doi: 10.18429/JACoW-IBIC2024-THP60

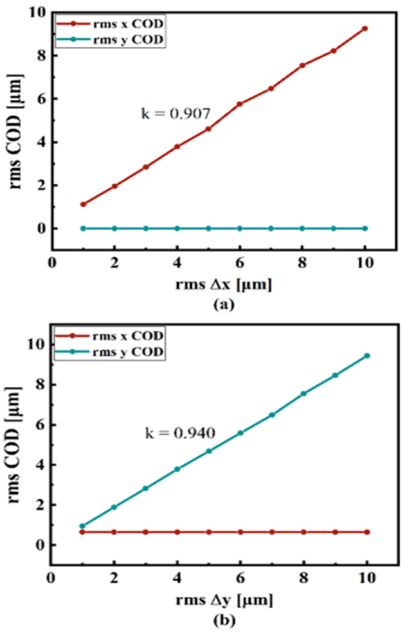

Figure 3: Effect of BPM displacement on HLS II COD: (a) COD caused by horizontal BPM displacement; (b) COD caused by vertical BPM displacement.

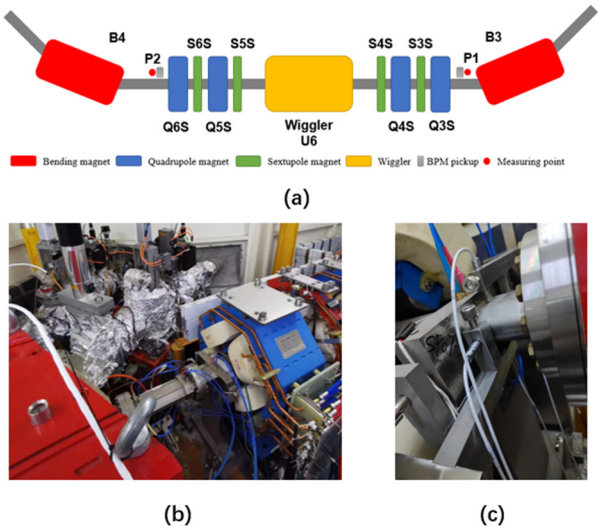

Figure 4: Installation of capacitive displacement measurement systems. (a) Installation location, (b) and (c) Photos of P1 and P2 at HLS II.

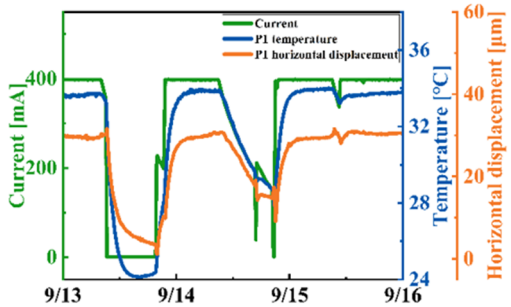

Figure 5: Horizontal displacement at P1.

DATA ANALYSIS

The displacement of BPM pickups is closely related to the movement of vacuum chamber and the displacement of BPM vacuum chamber is related to the beam current intensity, local temperature, overall ambient temperature, and overall motion of the storage ring vacuum chamber [5], as shown in Eq. (2), where, x_m represents the displacement of the vacuum chamber at location m, I represents the beam current intensity, T_m represents the temperature at location m, $T_{ambient}$ represents the ambient temperature and G represents the overall motion of the storage ring.

$$x_m = f(I, T_m, T_{ambient}, G) \tag{2}$$

The overall motion of the storage ring G can be viewed as a superposition of the motions at various points on the vacuum chamber, as shown in Eq. (3).

$$\begin{aligned} G &= \sum_{m=1}^{N} x_m = \sum_{m=1}^{N} f(I, T_m, T_{ambient}, G) \\ &= g(I, T_1, T_2, \cdots, T_N, T_{ambient}) \end{aligned} \tag{3}$$

By substituting Eq. (3) into Eq. (2), Eq. (4) is obtained. x_m is a function of beam current intensity, local temperature and ambient temperature. Thus, one set of beam current data, 64 sets of vacuum chamber temperatures, and two sets of ambient temperatures are used for predicting the displacement of BPM vacuum chambers. Normalization and threshold trigger algorithms are applied to the raw data to make the model converge as much as possible.

$$\begin{aligned} x_m &= f\big(I, T_m, T_{ambient}, g(I, T_1, T_2, \cdots, T_N, T_{ambient})\big) \\ &= f_1(I, T_1, T_2, \cdots, T_N, T_{ambient}) \end{aligned} \tag{4}$$

MACHINE LEARNING MODEL

Considering the time dependence of data, a machine learning model with gated recurrent units (GRU) is used to predict the displacement of vacuum chambers as well as BPM pickups. The model consists of 1 GRU layer and 4 fully connected layers. The mean square error (MSE) was selected as the cost function.

43200 sets of data were collected and was divided in training set, validation set and test set in the ratio of 38:1:1. Optuna [4] is used to optimize the hyperparameters including the structure parameters and learning rate of the model with training set and validation set. From the twenty sets of hyperparameters, the set with the smallest error was selected as the final structure of the model. The optimized structure of the neural network is shown in Fig. 6.

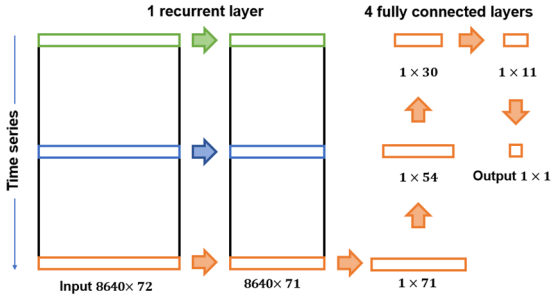

Figure 6: Structure of the model with GRU.

ISBN: 978-3-95450-249-3 ISSN: 2673-5350 doi: 10.18429/JACoW-IBIC2024-THP60

After training, the performance of the model on the test set in the horizontal plane at P1 and P2 is shown in Fig. 7 and Fig. 8. For the convenience of presentation, the data are categorized into three model: shutdown mode, injection mode and top-up mode. The MSE error in valid set is 0.1100 μm^2 and the MSE error in test set is 0.1221 μm^2, which is 349 nm. Such kind of work was also carried out at P1 and P2 in both horizontal and vertical plane. The results are shown in Table 2.

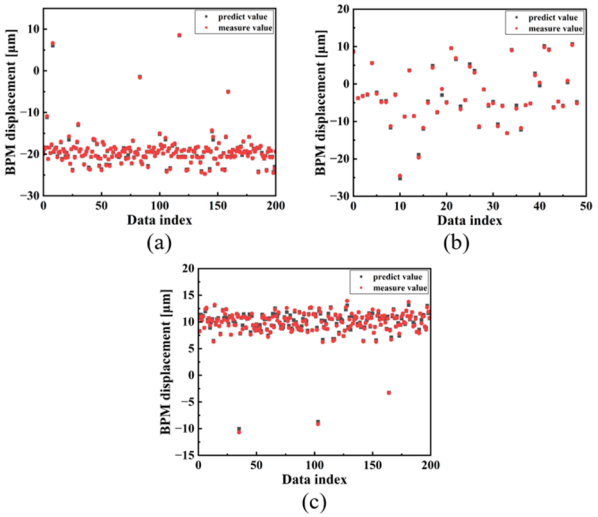

Figure 7: Predicted and measured values of the BPM displacement at P1 in the horizontal plane. (a) in the shutdown mode, (b) in the injection mode and (c) in the top-up mode.

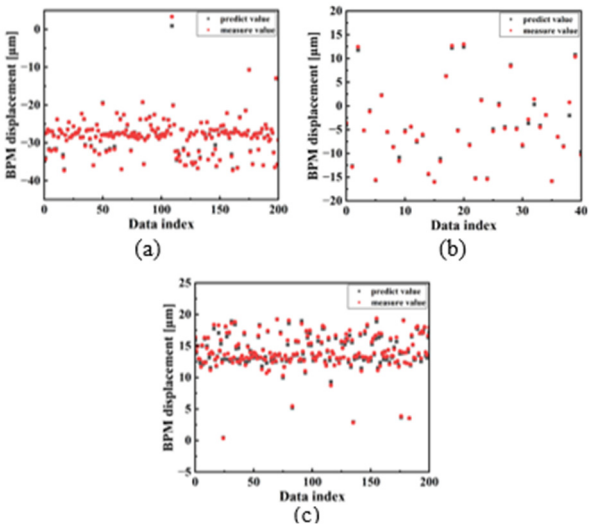

Figure 8: Predicted and measured values of the BPM displacement at P2 in the horizontal plane. (a) in the shutdown mode, (b) in the injection mode and (c) in the top-up mode.

Multilayer neural networks and convolutional neural networks (CNN) were also tested on this dataset. The structures of the two neural networks are shown in Fig. 9 and Fig. 10. The errors of the two models are shown in Table 3 and Table 4.

The multi-layer neural networks have 2 hidden layers and the activation function is selected as Selu. The multi-layer neural networks have better real-time performance and are fast to train as well as inference, which is especially important for CPU-only virtual machines. The RMSE of multilayer neural networks is about twice as high as that of the model with GRU. The error is acceptable for HLS II, while further optimization is still needed for HALF.

The model with CNN has 1 convolutional layer, 2 recurrent layers, 1 recurrent-skip layer and 1 fully connected layer. The convolutional layer is designed to learn the spatial relationship of the vacuum chamber deformation in the storage ring. however, the chambers are connected with bellows, and the spatial relationship between the data may not be significant. The training results also show that CNN error is slightly larger than the model with GRU.

Table 2: Errors of the Model with GRU

	Test set error (MSE)	**Test set error (RMSE)**
Horizontal displacement at P1	0.1221 μm^2	349 nm
Vertical displacement at P1	0.1043 μm^2	323 nm
Horizontal displacement at P2	0.1571 μm^2	396 nm
Vertical displacement at P2	0.0255 μm^2	160 nm

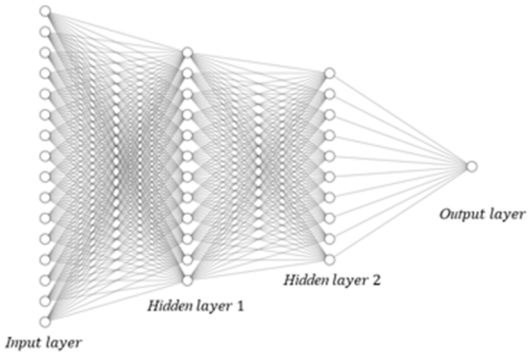

Figure 9: Structure of the multi-layer neural networks built for BPM displacement prediction.

Table 3: Errors of Multilayer Neural Networks

	Test set error (MSE)	**Test set error (RMSE)**
Horizontal displacement at P1	0.7579 μm^2	870.6 nm
Vertical displacement at P1	0.7164 μm^2	846.4 nm
Horizontal displacement at P2	0.4524 μm^2	672.6 nm
Vertical displacement at P2	0.0934 μm^2	305.6 nm

ISBN: 978-3-95450-249-3 ISSN: 2673-5350 doi: 10.18429/JACoW-IBIC2024-THP60

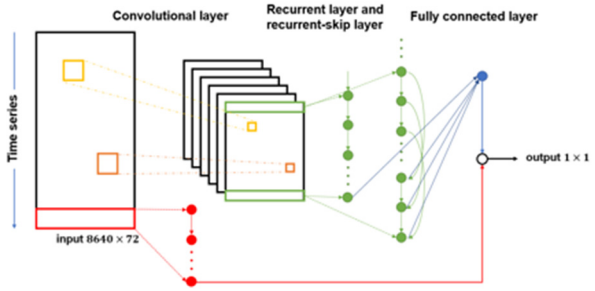

Figure 10: Structure of the model with CNN built for BPM displacement prediction.

Table 4: Errors of Model with CNN

	Test set error (MSE)	Test set error (RMSE)
Horizontal displacement at P1	0.2905 μm^2	539 nm
Vertical displacement at P1	0.2642 μm^2	514 nm
Horizontal displacement at P2	0.2970 μm^2	545 nm
Vertical displacement at P2	0.0745 μm^2	273 nm

CONCLUSION

In this article, the effects of BPM displacement on beam orbit stability were calculated for HLS II. Three types of neural networks are designed to predict the displacement of BPM displacement. The errors of all three models satisfy the requirements for BPM mechanical stability at HLS II.

All three machine learning models performed well on offline data, and we also attempted to use the models for online testing. An IOC for capacitive displacement measurement system and a soft IOC for machine learning models were built. Online testing will be conducted in the coming months.

ACKNOWLEDGEMENTS

Work supported by the National Natural Science Foundation of China under Grant No.12005223, 12075236. the Hefei Advanced Light Facility Pre-research Project, and the Hefei Advanced Light Facility Project.

REFERENCES

[1] L. Zhang. “Beam stability consideration for low emittance storage ring”, in workshop on ambient ground motion and vibration suppression for low emittance storage ring, GM2017, Beijing, China.

[2] R. Bartolini, H. C. Huang, J. Kay, and I. P. S. Martin, “Analysis of Beam Orbit Stability and Ground Vibrations at the Diamond Storage Ring”, in *Proc. 11th European Particle Accelerator Conf. (EPAC'08)*, Genoa, Italy, Jun. 2008, paper WEPC002, pp. 1980-1982.

[3] R. J. Steinhagen, “LHC beam stability and feedback control-orbit and energy”, 2007. No. CERN-AB-2007-049.

[4] Micro-Epsilon, `https://www.micro-epsilon.com`

[5] Takuya Akiba, Shotaro Sano, *et al*., “Optuna: A Next-generation Hyperparameter Optimization Framework”, in *the 25th ACM SIGKDD International Conference*, 2019, pp. 2623-2631. `doi:10.1145/3292500.3330701`